Cambridge Quantum

Noise-Aware Quantum Amplitude Estimation

by Steven Herbert, Roland Guichard, Darren Ng

Cambridge Quantum
Department of Computer Science and Technology,
University of Cambridge, United Kingdom
STEVEN HERBERT
steven.herbert@cambridgequantum.com

Cambridge Quantum
ROLAND GUICHARD
roland.guichard@cambridgequantum.com
DARREN NG
darren.ng@cambridgequantum.com

Cambridge Quantum
Terrington House
13-15 Hills Road
Cambridge CB2 1NL
United Kingdom

Published by Cambridge Quantum

10 September 2021

NOISE-AWARE QUANTUM AMPLITUDE ESTIMATION

STEVEN HERBERT[1,2], ROLAND GUICHARD[1] & DARREN NG[1]

[1] *Cambridge Quantum Computing Ltd, 9a Bridge Street, Cambridge, CB2 1UB, UK*
[2] *Department of Computer Science and Technology, University of Cambridge, UK*

Abstract. In this paper we derive from simple and reasonable assumptions a Gaussian noise model for NISQ Quantum Amplitude Estimation (QAE). We provide results from QAE run on various IBM superconducting quantum computers and Honeywell's H1 trapped-ion quantum computer to show that the proposed model is a good fit for real-world experimental data. We then give an example of how to embed this noise model into any NISQ QAE algorithm, such that the amplitude estimation is "noise-aware".

I. Introduction

The term *noisy intermediate-scale quantum [computer]* (NISQ), coined by John Preskill [1] has become the industry standard for early quantum computers, and the name immediately tells us two of their most important features: they are noisy, and they are too small ("intermediate-scale") to run fault-tolerant algorithms. Thus noise, and the consequent possibility of error, is something we have to live with.

Many ingenious suggestions for NISQ error *mitigation* (that is, using circuit design and classical pre- and post-processing to reduce the adverse effects of noise, without actually using any qubits for quantum error *correction*) have been proposed, including *zero-noise extrapolation* [2, 3], *randomised compilation* [4], *probabilistic error correction* [5] and many more. It is also likely that some quantum error correction (albeit falling short of the amount required for fault-tolerance) will ultimately be deployed in NISQ algorithms (*e.g.*, Refs. [6, 7]). An alternative, and in general complementary, approach is to characterise the noise as a "noise model" and handle the noise at the application level. This approach is particularly applicable for quantum sampling algorithms (*e.g.* Refs. [8–11]), where the effect of the noise is that the samples are from a different distribution than in the corresponding noiseless case, but in principle with an accurate noise model the distribution actually being sampled from can still be expressed. Moreover, sampling provides the basis for many quantum optimisation and estimation algorithms [8, 9], and with an accurate noise model there may still be quantum advantage in speed of convergence even in the presence of noise (that is, if the noise is sufficiently mild, with some errors possibly having been mitigated / corrected by some of the techniques mentioned).

In this paper we address what is probably the simplest such instance of this concept, by proposing a suitable model for the noise accumulated when Grover iterations are repeated to perform quantum amplitude amplification. In particular, we address one such algorithm, quantum amplitude estimation (QAE), and focus on propositions for NISQ QAE, which do not call quantum phase estimation as a subroutine [12–15]. Thus, in these algorithms the quantum circuits consist only of state preparation and then amplitude amplification, there is no other circuitry involved. Moreover, these proposed algorithms all share the property that only a single qubit is measured, which gives us the basis for a simple Gaussian noise model. Additionally, QAE not only provides a suitable subject for a noise model, but is also an important NISQ algorithm which underpins quantum Monte Carlo integration (QMCI) [8, 16–18], and thus forms the basis for many important anticipated applications in, for example, quantum finance [19–29].

This approach of translating the noise at the physical level to the resultant effect on the estimation accuracy at the application level in QAE has begun to gain traction in recent months, with both Brown *et al* [30] and Tanaka *et al* [31] investigating how generic noise models such as depolarising, amplitude damping and phase damping noise impact the performance of *Amplitude Estimation without Phase Estimation* [12]. The results we present in this paper are complementary to, and in some ways extend, these results. In particular, to our knowledge this is the first time that a noise model specific to QAE has been derived, even though the aforementioned papers note the importance (and difficulty) of doing so ("It is indeed a difficult challenge to model a noise effect" Ref. [31, Section 5]; "... any lack of accuracy in one's noise characterisation will translate to a lack of accuracy in amplitude estimation. Understanding better this difficulty represents a fruitful line of future research." Ref. [30, Section IV-A]). Moreover, a

Contact: Steven.Herbert@cambridgequantum.com

noise model is a statistical characterisation of some physical process, and hence stands independently of any particular flavour of QAE, and instead provides a quantification of the measurement uncertainty that can then be used to more accurately infer the amplitude from the measured data. To this end, our main example for how to use the proposed noise model to achieve noise-aware QAE concerns a quantification of the number of additional shots that are needed, given the circuit depth, to achieve the same variance as the noiseless case. This applies to any NISQ QAE where repeated shots of the same circuit are used to infer the amplitude, including some recent suggestions for shallow-depth QAE [32, 33].

Looking more broadly at NISQ QAE, Wang *et al* [34] take a different approach and cast QAE as an instance of generic observable measurement. They take an adaptive, Bayesian approach, showing that by tuning the circuit parameters adaptively as the parameters become known with greater confidence, in turn the future expected information gain can be maximised. In future work it will be interesting to see if, and to what extent, the bespoke noise model we propose here can further enhance the Bayesian approach to quantum sampling – however this is beyond the scope of the present paper. It is also worth noting that efforts are afoot to investigate the performance of QAE on noisy quantum computers, even without application-level handling of the noise [35].

The remainder of the paper is organised as follows: in Section II we describe in detail how the Gaussian noise model is derived from some reasonable initial assumptions – and also demonstrate that the noise model leads to the expected asymptotic behaviour; in Section III we present a series of experiments, run on actual quantum hardware, to probe the real-world applicability of our proposed noise-model; then in Section IV we include and discuss the results of these experiments; in Section V we give the simple example of noise-aware QAE; in Section VI we give some further numerical results for noise-aware QAE; and finally in Section VII we draw conclusions.

II. Theoretical Derivation of the Gaussian Noise Model

To derive the Gaussian noise model, it is first necessary to introduce QAE [36]: QAE uses a generalisation of Grover's search algorithm [37], amplitude amplification, to estimate the amplitude, $a = \sin^2\theta$, of a general n-qubit quantum state expressed in the form:

$$|\psi\rangle = \cos\theta\,|\Psi_0\rangle\,|0\rangle + \sin\theta\,|\Psi_1\rangle\,|1\rangle \tag{1}$$

for some $(n-1)$-qubit states $|\Psi_0\rangle$ and $|\Psi_1\rangle$. A circuit, A, which prepares $|\psi\rangle$, that is $|\psi\rangle = A\,|0^n\rangle$, is taken as the input to the QAE algorithm, from which it is possible to build an operator $Q = -AS_0A^{-1}S_\chi$ (where $S_0 = X^{\otimes n}(C_{n-1}Z)X^{\otimes n}$ and $S_\chi = I_{2^{n-1}} \otimes Z$ do not depend on A) which performs Grover iteration:

$$Q^m\,|\psi\rangle = \cos((2m+1)\theta)|\Psi_0\rangle|0\rangle + \sin((2m+1)\theta)|\Psi_1\rangle|1\rangle \tag{2}$$

Thus, for m applications of Q, the probability of measuring the state $|1\rangle$ on the last qubit is $\sin^2((2m+1)\theta)$, and the essential idea common to all NISQ QAE algorithms is to run circuits for a variety of different values of m and then to use classical post-processing to estimate θ and hence a. In the presence of noise each Grover iterate will not necessarily enact a rotation of exactly 2θ and thus we can write the actual rotation enacted by the i^{th} Grover iterate as $2\theta + \epsilon_i$ where ϵ_i is some error, which then gives:

$$\begin{aligned}|\psi\rangle \xrightarrow{Q^m} &\cos\left((2m+1)\,\theta + \sum_{i=1}^{m}\epsilon_i\right)|\Psi_0\rangle\,|0\rangle \\ &+ \sin\left((2m+1)\,\theta + \sum_{i=1}^{m}\epsilon_i\right)|\Psi_1\rangle\,|1\rangle\end{aligned} \tag{3}$$

Note that Equation (3) is a general expression for the state after m Grover iterations: that is, there are no hidden assumptions in treating each Grover iteration to be a rotation by the desired (noiseless) angle plus some additional erroneous component – this is a completely general way of representing the final state of a QAE circuit run on a noisy machine. It is also pertinent that, by treating the Grover iteration as a "black box" in this way, Equation (3) is agnostic to the specific realisation of the algorithm as a quantum circuit – covering even cases where quantum error correction is deployed, for example. In order to turn this into a useful noise model it is necessary to introduce an assumption, namely that the various ϵ_i are independent and identically distributed (i.i.d.) and m is sufficiently large that we can invoke the central limit theorem (CLT) to approximate the sum of the random variables ϵ_i as a single random variable drawn from a Gaussian distribution. In this case that the state can be expressed:

$$\begin{aligned}Q^m\,|\psi\rangle = &\cos((2m+1)\theta + \theta_\epsilon)\,|\Psi_0\rangle\,|0\rangle \\ &+ \sin((2m+1)\theta + \theta_\epsilon)\,|\Psi_1\rangle\,|1\rangle\end{aligned} \tag{4}$$

such that $\theta_\epsilon \sim \mathcal{N}(k_\mu m, k_\sigma m)$, where $\mathcal{N}(\text{mean,variance})$ is the normal distribution, and k_μ and k_σ are constants. It is worth noting that the assumption that the various ϵ_i are i.i.d. is actually an unnecessarily strong requirement. In fact, all that is required is

that a sufficiently large number of independent underlying "factors" contribute to the randomness that a Gaussian random variable well-models the value in question. This assumption is identical to that ubiquitously used in wireless communications literature to model noise as *additive white Gaussian noise* [38].

This noise model applies because we are only interested in the error on a single qubit, and this allows us to use a classically inspired approach and invoke the CLT. The result is a noise model that is somewhat different in appearance to that which may conventionally be derived for modelling noisy quantum channels. In particular, we do not express a mixed state, but rather notice that a mixed state simply captures classical uncertainty about which pure state some quantum system is in. Thus our proposed Gaussian noise model can be thought of as always treating the quantum state as pure, and then quantifying the relevant part of our uncertainty about what that quantum state is separately.

II.1. **Relationship between the Gaussian noise model and depolarising noise.** Of the existing generic noise models, our proposed Gaussian noise model is most similar to the depolarising noise model. The depolarising noise model supposes that each layer of quantum gates has some probability of completely depolarising the quantum state, whereas the Gaussian noise model supposes that the state gradually depolarises in a continuous manner. An important feature of the depolarising channel is that the state tends towards the maximally mixed state exponentially fast, that is the probability of measuring zero is:

$$p(0) = p_{coh}^{d}\cos^2((2m+1)\theta) + (1-p_{coh}^{d})\frac{1}{2} \qquad (5)$$

where p_{coh} is some (fixed) finite probability of the state remaining coherent (not depolarising), and d is the circuit depth. For comparison with the Gaussian noise model it is easiest to express the probability of measuring 1 subtracted from the probability of measuring 0. Using the fact that the circuit depth is approximately proportional to m we get:

$$\begin{aligned} p(0)-p(1) &= \left(\tilde{p}_{coh}^{m}\cos^2((2m+1)\theta)+(1-\tilde{p}_{coh}^{m})\frac{1}{2}\right) \\ &\quad -\left(\tilde{p}_{coh}^{m}\sin^2((2m+1)\theta)+(1-\tilde{p}_{coh}^{m})\frac{1}{2}\right) \\ &= \tilde{p}_{coh}^{m}\left(\cos^2((2m+1)\theta)-\sin^2((2m+1)\theta)\right) \end{aligned} \qquad (6)$$

where $\tilde{p}_{coh}$ is an adjusted version of p_{coh} such that the scaling is in terms of number of Grover iterates (approximately proportional to circuit depth). We will now show that the same asymptotic behaviour occurs in the proposed Gaussian noise model. To do so, first we consider the probability of the measurement outcome being 0 when the noise is Gaussian, which can be expressed:

$$\begin{aligned} p(0) &= \int_{-\infty}^{\infty} p(0|\theta_\epsilon)p(\theta_\epsilon)\,\mathrm{d}\theta_\epsilon \\ &= \int_{-\infty}^{\infty} \cos^2((2m+1)\theta+\theta_\epsilon)\frac{e^{-\frac{(\theta_\epsilon-k_\mu m)^2}{2k_\sigma m}}}{\sqrt{2\pi k_\sigma m}}\,\mathrm{d}\theta_\epsilon \end{aligned} \qquad (7)$$

We can similarly express the probability of outcome 1:

$$p(1) = \int_{-\infty}^{\infty} \sin^2((2m+1)\theta+\theta_\epsilon)\frac{e^{-\frac{(\theta_\epsilon-k_\mu m)^2}{2k_\sigma m}}}{\sqrt{2\pi k_\sigma m}}\,\mathrm{d}\theta_\epsilon \qquad (8)$$

Next we subtract (8) from (7):

$$\begin{aligned} p(0)-p(1) &= \int_{-\infty}^{\infty} \cos^2((2m+1)\theta+\theta_\epsilon)\frac{e^{-\frac{(\theta_\epsilon-k_\mu m)^2}{2k_\sigma m}}}{\sqrt{2\pi k_\sigma m}} \\ &\quad -\sin^2((2m+1)\theta+\theta_\epsilon)\frac{e^{-\frac{(\theta_\epsilon-k_\mu m)^2}{2k_\sigma m}}}{\sqrt{2\pi k_\sigma m}}\,\mathrm{d}\theta_\epsilon \\ &= \frac{1}{\sqrt{2\pi k_\sigma m}}\int_{-\infty}^{\infty}\cos\left(2\left((2m+1)\theta+\theta_\epsilon\right)\right) \\ &\quad e^{-\frac{(\theta_\epsilon-k_\mu m)^2}{2k_\sigma m}}\,\mathrm{d}\theta_\epsilon \\ &= \frac{1}{\sqrt{2\pi k_\sigma m}} \\ &\quad \mathcal{R}\left(e^{2i(2m+1)\theta}\int_{-\infty}^{\infty} e^{2i\theta_\epsilon}e^{-\frac{(\theta_\epsilon-k_\mu m)^2}{2k_\sigma m}}\,\mathrm{d}\theta_\epsilon\right) \\ &= \frac{1}{\sqrt{2\pi k_\sigma m}} \\ &\quad \mathcal{R}\left(e^{2i(2m+1)\theta+2ik_\mu m}\int_{-\infty}^{\infty} e^{2i\tilde{\theta}_\epsilon-\frac{\tilde{\theta}_\epsilon^2}{2k_\sigma m}}\,\mathrm{d}\tilde{\theta}_\epsilon\right) \\ &= \frac{1}{\sqrt{2\pi k_\sigma m}} \\ &\quad \mathcal{R}\left(e^{2i(2m+1)\theta+2ik_\mu m}\sqrt{2\pi k_\sigma m}\,e^{-2k_\sigma m}\right) \\ &= e^{-2k_\sigma m}\cos(2((2m+1)\theta+k_\mu m)) \\ &= e^{-2k_\sigma m}\Big(\cos^2((2m+1)\theta+k_\mu m) \\ &\quad -\sin^2((2m+1)\theta+k_\mu m)\Big) \end{aligned} \qquad (9)$$

where $\mathcal{R}$ denotes the real part, and the substitution $\tilde{\theta}_\epsilon = \theta_\epsilon - k_\mu m$ is used to simplify the integral.

We can see that when $k_\mu = 0$ (which is effectively implicit in the depolarising noise model) the asymptotic behaviour is consistent with that of the depolarising channel, (6). This is important as a proposed noise model which did not have the property of tending to the maximally mixed state exponentially

quickly would be unlikely to be correct or useful. Furthermore, we can see that for "zero" depth circuits ($m = 0$) we have that $p(0) - p(1) = \cos^2\theta - \sin^2\theta$, and so in the zero-depth limit the measurement outcome probabilities correspond to those of the noiseless case, as we would expect.

III. Experimental Set-up

In order to gather experimental results to assess the real-world applicability of the proposed Gaussian noise model, it is necessary to select some state preparation circuits, A, and run QAE on real quantum hardware. For this, we are guided by the following two principles: firstly, we minimise the number of qubits used in A in order that we can run deeper circuits (more applications of Q) which thus allows us to better observe how well the Gaussian noise model fits the experimental data; and secondly we choose circuits which have the property that noiselessly θ is such that on periodic numbers of Grover iterations the measurement outcome is either $|0\rangle$ or $|1\rangle$ with certainty, which allows us to display plots to illustrate how well the noise model fits the experimental data. Two circuits which achieve these aims are A_1 and A_2, shown in Fig. 1, which prepare the states:

$$A_1|00\rangle = \cos(\pi/6)|\Psi_0\rangle|0\rangle + \sin(\pi/6)|\Psi_1\rangle|1\rangle \quad (10)$$

$$A_2|00\rangle = \cos(\pi/3)|\Psi_0\rangle|0\rangle + \sin(\pi/3)|\Psi_1\rangle|1\rangle \quad (11)$$

So we can see that

$$Q_1^m A_1|00\rangle = \cos((2m+1)\pi/6)|\Psi_0\rangle|0\rangle + \sin((2m+1)\pi/6)|\Psi_1\rangle|1\rangle \quad (12)$$

$$Q_2^m A_2|00\rangle = \cos((2m+1)\pi/3)|\Psi_0\rangle|0\rangle + \sin((2m+1)\pi/3)|\Psi_1\rangle|1\rangle \quad (13)$$

where Q_1 and Q_2 are the Grover iterate circuits for A_1 and A_2 respectively. We can see that $Q_1^m A_1|00\rangle$ (resp. $Q_2^m A_2|00\rangle$) has the property that the measurement of the last qubit is 1 (resp. 0) with certainty when $(m-1) \mod 3 = 0$ (that is for $m = 1, 4, 7, ...$). Fig. 2 illustrates this for the case of A_1. Even though in principle QAE could be applied to a single-qubit circuit, A, the lack of entanglement therein would make it an unsuitable experiment, and thus by selecting 2 qubit circuits, we have used the minimum number of qubits that we can reasonably expect to lead to meaningful results.

Whilst A_1 and A_2 achieve our aim of running simple circuits that lead to results that can readily be plotted, it is also beneficial to include a range of different circuits. To this end we also run QAE for A_1 and A_2 simultaneously (to introduce the possibility of cross-talk) and additionally for A_3, A_4 and A_5, also

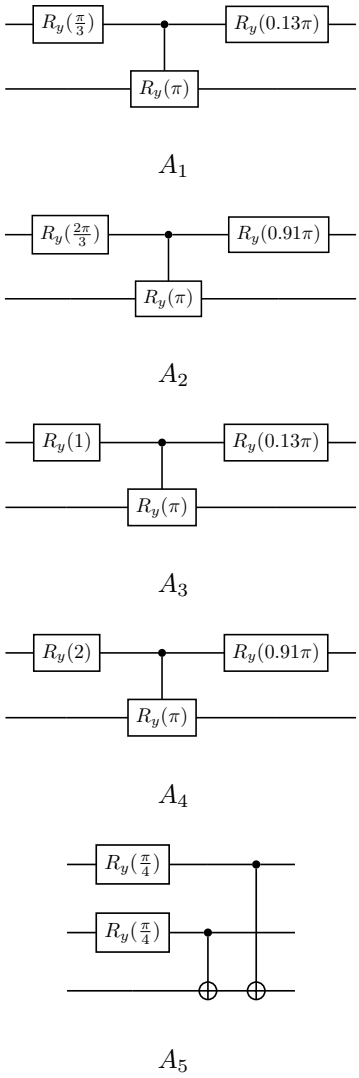

Fig. 1. State preparation circuits.

shown in Fig. 1, which prepare the states:

$$A_3|00\rangle = \cos(1/2)|\Psi_0\rangle|0\rangle + \sin(1/2)|\Psi_1\rangle|1\rangle \quad (14)$$

$$A_4|00\rangle = \cos(1)|\Psi_0\rangle|0\rangle + \sin(1)|\Psi_1\rangle|1\rangle \quad (15)$$

A_3 and A_4 are such that the final qubit does not align with the $|0\rangle$ or $|1\rangle$ axes after any number of applications of Q.

For the first round of experiments, we ran the QAE circuits for m applications of Q where $m = 0 \ldots 67$. This range were set on the basis of preliminary studies to discover the reasonable maximum circuit depths (*i.e.* before noise becomes overwhelming). For the experiments we used four of IBMs five-qubit machines (Athens, Bogota, Rome and Santiago – all of the five-qubit machines online at the time of the experiments), each of which uses superconducting qubits connected in a line [39]. Cambridge Quantum

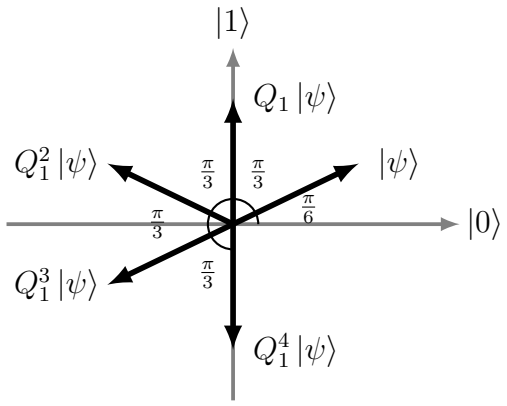

Fig. 2. Illustration of the action of Q_1^m on $|\psi\rangle = A_1|00\rangle$. Here we show for $m = 0 \ldots 4$, but we can easily see that the pattern will repeat after $m = 6$ (*i.e.* so that we can take m modulo 6 to find the rotation angle).

Computing's tket compiler [40] was used to run the circuits – the compiler was set to map the circuit to the physical qubit connectivity and native gate-set but not to perform any "optimisation", that is circuit re-writing to achieve a functionally equivalent but shallow-depth circuit (compiled circuits shown in Appendix A). In this way, we guaranteed that the circuit executed consisted of the appropriate number of repeated Grover iterations, as is necessary to probe the validity of the proposed noise model.

We used minimum mean-squared error (MMSE) parameter fitting to find the noise-model parameters that best fit the experimental data. For each experiment we did this for three noise models: the Gaussian noise model proposed herein; the proposed Gaussian noise model with mean set to zero (*i.e.* not a variable parameter) and the depolarising noise model (as previously identified, the closest of the existing, generic noise models). We ran each circuit for the maximum allowed number of shots, which is 8192. By doing so we were able to simplify the analysis by treating the average of the 8192 shots as exactly equal to the square of the modulus of the amplitude of the $|1\rangle$ component of the last qubit (that is, when expressed in the form of Eqn. (2)).

To see why this holds let $\hat{p}_1$ be the estimate of p_1 we obtain by averaging 8192 shots, then we have that:

$$\hat{p}_1 \sim \mathcal{N}(p_1, p_1(1-p_1)/8192) \tag{16}$$

using the Gaussian approximation of the binomial (which is clearly valid for the summation of 8192 i.i.d Bernoulli random variables). The standard deviation (square-root of variance) is maximised when $p_1 = 0.5$ which we use to find that the standard-deviation is at most 0.00552, which is extremely small, and means that it is reasonable to use the average of the 8192 shots as exactly p_1 in the following analysis.

For the second round of experiments we used Honeywell's H1 trapped-ion quantum computer [41]. Owing to the slower gate times, and more restricted device availability, we were only able to run a smaller measurement campaign than that using the IBM devices. However, because of the superior quantum volume of the Honeywell machine compared to the IBM devices [42], we were able to confidently run a three qubit circuit, A_5, also shown in Fig. 1, which prepares the state:

$$A_5|000\rangle = \cos(\pi/6)|\Psi_0\rangle|0\rangle + \sin(\pi/6)|\Psi_1\rangle|1\rangle \tag{17}$$

A_5 has the same "periodic" property as A_1 that noiselessly $Q^m A_5|000\rangle$ yields measurement outcome 1 with certainty on the third qubit when $(m-1) \mod 3 = 0$. Experiments were run for $m = 0, 1, \ldots 12$, and for each circuit, 1024 shots were performed. On a different day, further experiments were run on the Honeywell machine for $m = 0, 1, \ldots 13$, and for each circuit, 1500 shots were performed. Whilst these numbers of shots are approximately an order of magnitude smaller than in the IBM experiments, it remains acceptable for the argument about neglecting the binomial uncertainty to still hold. The two different rounds of experiments on the Honeywell machine are denoted "(i)" and "(ii)" respectively in the following.

IV. Results and Discussion

From the MMSE-fitted parameters we calculate R^2 values to evaluate the goodness-of-fit of the three noise models under consideration. These R^2 values are given in Table 1 – note that R^2 is at most equal to 1 and $R^2 = 1$ means that all of the experimentally observed variance is explained by the proposed model. Additionally Fig. 3 shows plots for A_1 run on the various IBM machines, with circuit depths $m = 1, 4, 7, \ldots$ (*i.e.* number of Grover iterates such that the noiseless measurement outcome is always equal to 1); and Fig. 4 shows plots for A_1 run on the various machines, with circuit depths $m = 0, 2, 3, 5, 6, 8, 9, \ldots$ (*i.e.* number of Grover iterates such that the noiseless measurement outcome is equal to zero with probability 0.75).

From these results it is immediately apparent that, as emphasised by the bold font in Table 1, the proposed Gaussian noise model (with variable mean) is invariably a better fit than either the Gaussian noise model with mean set to zero, or the depolarising noise model. This is because the Gaussian noise model with parameterised mean can capture a constant "bias" or "drift" where each Grover iterate performs a rotation

Circuit	Machine	Gaussian	Gaussian (zero mean)	Depolarising
A_1	Athens	**0.9546**	0.8052	0.8052
	Bogota	**0.9400**	0.5822	0.5822
	Rome	**0.9667**	0.8678	0.8678
	Santiago	**0.8936**	0.8721	0.8721
A_2	Athens	**0.8821**	0.7741	0.7741
	Bogota	**0.8633**	0.7857	0.7857
	Rome	**0.6658**	0.6323	0.6323
	Santiago	**0.8956**	0.8953	0.8952
A_1'	Athens	**0.8967**	0.8893	0.8893
	Bogota	**0.8138**	0.7584	0.7584
	Rome	**0.5066**	0.5063	0.5061
	Santiago	**0.7664**	0.7115	0.7115
A_2'	Athens	**0.9110**	0.8398	0.8398
	Bogota	**0.7283**	0.6659	0.6659
	Rome	**0.8089**	0.8080	0.8072
	Santiago	**0.7975**	0.7884	0.7884
A_3	Athens	**0.9899**	0.9831	0.9831
	Bogota	**0.7763**	0.6744	0.6743
	Rome	**0.8890**	0.6121	0.6121
	Santiago	**0.9260**	0.8638	0.8638
A_4	Athens	**0.8876**	0.8527	0.8527
	Bogota	**0.8755**	0.8038	0.8038
	Rome	**0.8040**	0.7290	0.7290
	Santiago	**0.8619**	0.8179	0.8179
A_5	Honeywell H1 (i)	**0.9846**	0.9841	0.9841
	Honeywell H1 (ii)	**0.9671**	0.9612	0.9612

Table 1. R^2 values for the various state preparation circuits running on each of the 5-qubit IBM superconducting quantum computers and Honeywell's H1 trapped-ion quantum computer. A_1' and A_2' denote the results from A_1 and A_2 respectively when A_1 and A_2 were run simultaneously.

which is offset from the theoretical rotation angle by some constant amount (plus some zero-mean random noise). The results for rotation angles $\pi/6$ or $\pi/3$ (as in A_1, A_2 and A_5) clearly illustrate this, as the constant offset is manifested as the probability of measuring zero (or one) being alternately higher and lower (as the number of Grover iterations is incremented) than the simple depolarising case, as shown in Fig. 4 (specifically, Fig. 4 illustrates that noiselessly for all m such that $(m-1) \mod 3 \neq 0$ the probability of measurement outcome being $|0\rangle$ is 0.75). To see an example of this effect, consider the case of a small positive offset to the rotations in Fig. 2. In the case of Q^2 this offset would move the superposition closer to the direction $-|0\rangle$, and so there would a corresponding increase in the probability of measuring 0; conversely, in the case of Q^3 the offset would move the superposition closer to the direction $-|1\rangle$, and so there would be a corresponding increase in the probability of measuring 1. Thus we can see the grounds for the oscillation observed in Fig. 4. Most strikingly, for A_1 run on Bogota the Gaussian noise model (with variable mean) has $R^2 = 0.9400$ – thus explaining almost all of the experimental data – whereas the other two models have a much lower R^2 of 0.5822. It should also be noted that, whilst less amenable to visualisation, the same principle explains the better fit of the Gaussian noise model with parameterised mean for A_3 and A_4.

We can also see that in general the Gaussian noise model is a good fit for the the larger 3-qubit circuit, A_5. Here we have results from Honeywell – a fundamentally different physical manifestation of quantum computation – whose errors also seem to be reasonably well-captured by the Gaussian noise model, as illustrated also in Fig. 5. Note that the R^2 values

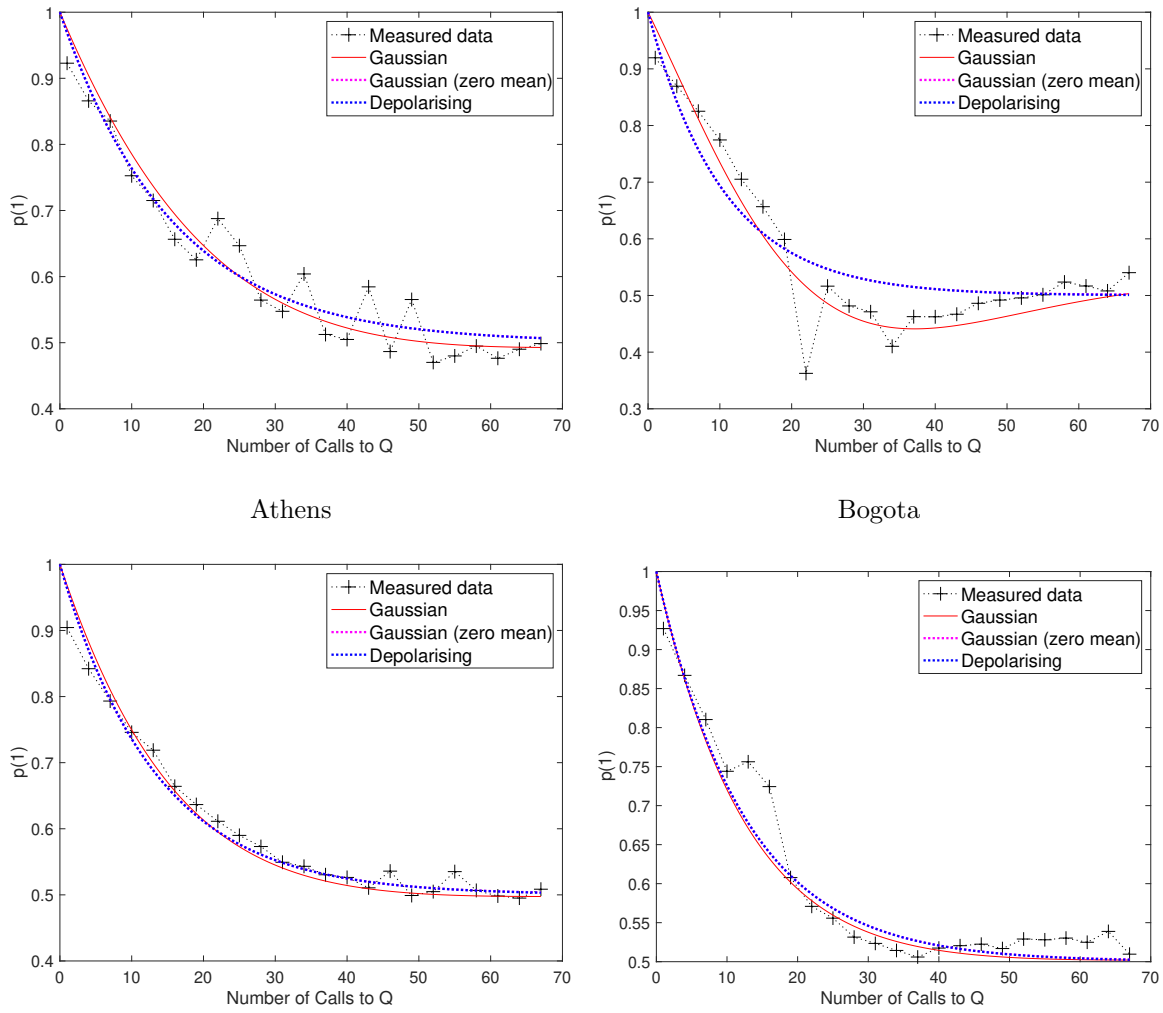

Fig. 3. A_1 run on each of the four 5-qubit IBM machines: results plotted for $1, 4, 7, \ldots$ Grover iterations (that is, iterations where in the absence of noise the measurement outcome would be 1 with certainty).

are consistently higher than those for the superconducting quantum computers owing to the fact that the circuits run were much less deep (there was "less variation to be explained").

To further analyse the results, there is merit in discussing the goodness-of-fit of the proposed Gaussian noise model from both a phenomenological and operational point of view. Regarding the former, the predictions of the noise model clearly do not explain *all* of the variation observed in the experimental data (that would correspond to $R^2 = 1$ for all experiments), and thus we can conclude that there are underlying physical causes of the variation not captured by the model. It is worth remarking that the fact that the proposed Gaussian noise model does not capture *everything* is to be expected, as the experiments were explicitly designed to capture raw data from the quantum hardware, and so do not even accommodate the correction of "state preparation and measurement" (SPAM) errors, for instance.

Indeed, Fig. 6 shows the two occasions when the R^2 value is particularly low, and SPAM error is a plausible explanation for each. In the case of A_2 on Rome, we can see that the experimental data does not converge to $p(0) = 0.5$ as the number of Grover iterations grows large – a property of all three of the noise models being considered (as the state after a large number of Grover iterations will be close to maximally mixed). One possible explanation for this (there could be others) is that there is a readout

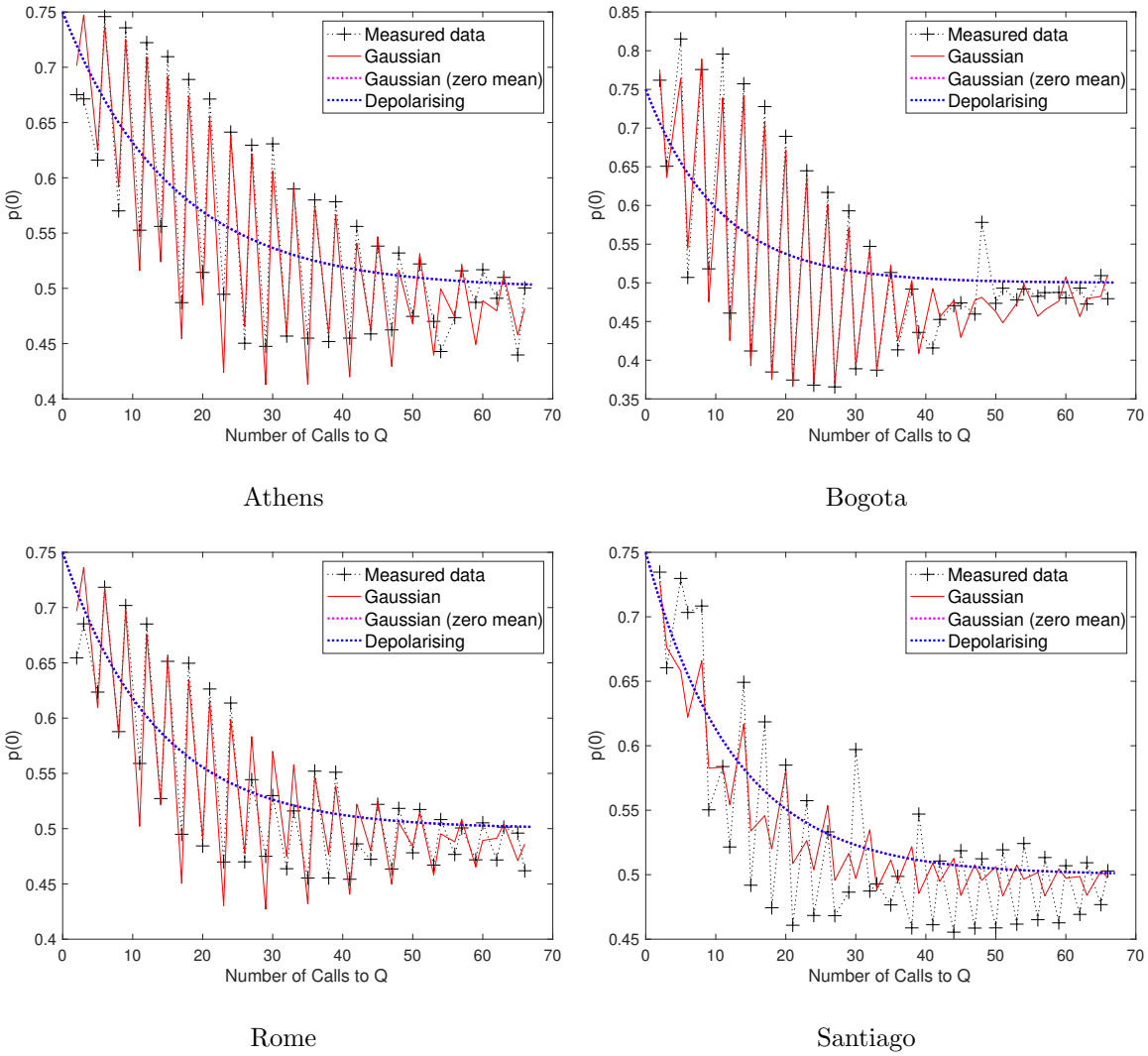

Fig. 4. A_1 run on each of the four 5-qubit IBM machines: results plotted for $2, 3, 5, 6, \ldots$ Grover iterations (that is, iterations where in the absence of noise the measurement outcome would be 0 exactly 0.75 of the time).

error, where (in this case) a bit-flip from 1 to 0 is more likely than the converse – which can be thought of as a type of SPAM error. In the case of A_1' on Rome, even for a shallow circuit that does little more than simply prepare and measure a state, we have that $p(1) = 0.7$ rather than ≈ 1, so clearly – indeed, almost by definition – there is a SPAM error.

We now turn to the operational benefits of the Gaussian noise model, which are twofold. Firstly, the fact that the proposed noise model *does* capture the bias is likely to be important for calibration – and furthermore calibration is very important in QAE, as a constant bias cannot be observed (that is, as we are trying to estimate the angle θ from which the amplitude can be found, if θ is perturbed by some constant offset, θ_c, then QAE will simply return the value of $\sin^2(\theta + \theta_c)$ – and no increase to the number of shots will change this). Secondly, we note that the Gaussian noise model is parameterised in a way that can readily be used in the application – as expounded on in detail in the next two sections. This corresponds to our original motivation to model the noise such that it can be handled at the application level.

It is also worth remarking further on the similarity between the depolarising noise model and the Gaussian noise model with mean set to zero: for all of the plots shown the curves for these are almost exactly one on top of the other; and this is reinforced by the R^2 values in Table 1 being almost exactly equal,

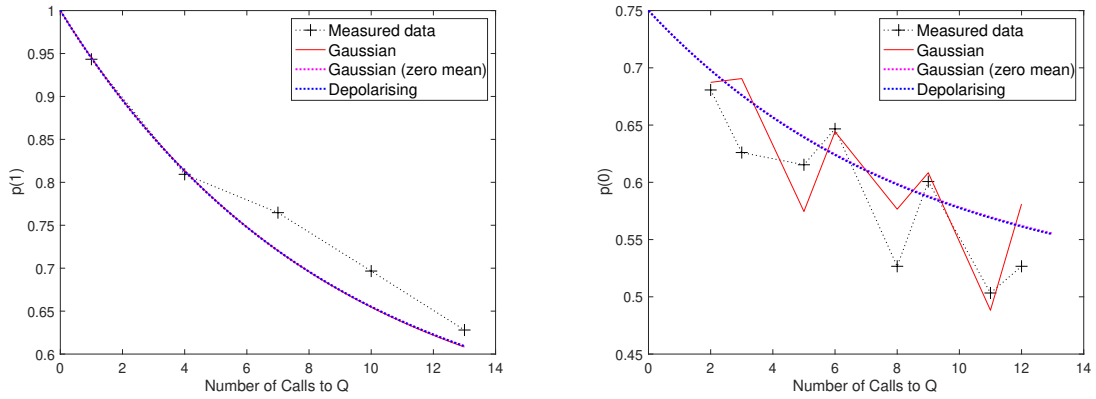

(a) (b)

Fig. 5. A_5 run on Honeywell H1 (ii): (a) results plotted for $1, 4, 7, \ldots$ Grover iterations (that is, iterations where in the absence of noise the measurement outcome would be 1 with certainty); (b) results plotted for $2, 3, 5, 6, \ldots$ Grover iterations (that is, iterations where in the absence of noise the measurement outcome would be 0 exactly 0.75 of the time).

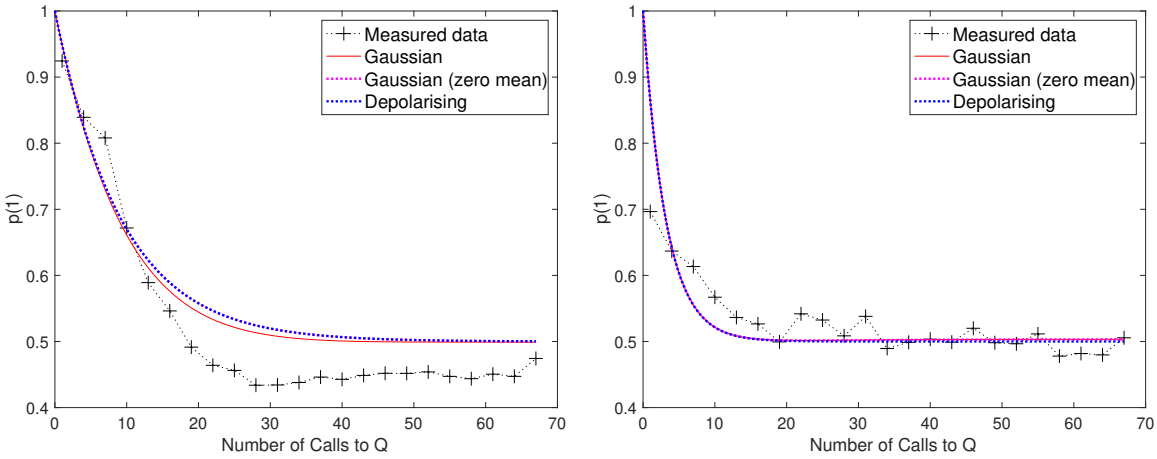

A_2 on Rome $(1, 4, 7, \ldots$ iterations) A_1' on Rome $(1, 4, 7, \ldots$ iterations)

Fig. 6. Plots for occasions when R^2 indicates that the Gaussian noise model is a poor fit.

even to four decimal places. In light of the asymptotic equivalence detailed in Section II.1, which can be seen to be an exact equivalence in the zero-mean case, it is unsurprising that there is *some* similarity between the two, but this level of agreement is unexpected – given that entirely different parameterised models were fitted to the experimental data. However, we can further use this fact – that depolarising noise is also a good experimental fit when the bias does not exist or has been corrected – to our advantage, which we indeed do in our noise-aware QAE.

V. Noise-Aware QAE: Theory

We now turn our attention to how this noise model can be used to improve our amplitude estimates. In particular, we show how the Gaussian noise model can be used to derive a rule for the necessary factor increase in the number of shots required to counteract the noise at a certain circuit depth. To do this, we assume that, even at the maximum circuit depth, the error θ_ϵ is a "small angle"; and also that $k_\mu = 0$ (something that could in principle be achieved by calibration of the machine) and k_σ is known from prior noise estimation.

Consider that the measurement outcome for a single shot of a circuit with some m Grover iterations is Bernoulli distributed with parameter $\sin^2((2m+1)\theta + \theta_\epsilon)$, using the aforementioned small angle assumption we get:

$$\begin{aligned}\sin^2((2m+1)\theta+\theta_\epsilon) =& \frac{1-\cos(2((2m+1)\theta+\theta_\epsilon))}{2} \\ =& \frac{1}{2}\Big(1-\cos(2(2m+1)\theta)\cos(2\theta_\epsilon) \\ &+\sin(2(2m+1)\theta)\sin(2\theta_\epsilon)\Big) \\ \approx& \frac{1}{2}\Big(1-\cos(2(2m+1)\theta) \\ &+2\theta_\epsilon\sin(2(2m+1)\theta)\Big) \\ =& \sin^2((2m+1)\theta) \\ &+\theta_\epsilon\sin(2(2m+1)\theta)\end{aligned} \tag{18}$$

Next we note that, by the Gaussian noise model, θ_ϵ is normally distributed, with zero mean (by the previous assumption of calibration), and variance $k_\sigma m$, and because $\sin(2(2m+1)\theta)$ is a constant whose magnitude is at most equal to one, it therefore follows that $\theta_\epsilon \sin(2(2m+1)\theta)$ is also normally distributed:

$$\theta_\epsilon \sin(2(2m+1)\theta) \sim \mathcal{N}(0, \sigma^2) \tag{19}$$

where $\sigma^2 \leq k_\sigma m$.

Next we let $\alpha_m = \sin^2((2m+1)\theta)$ be the amplitude of the qubit after m Grover iterates, and let N_m be the number of shots of this circuit. There are various ways in which the measurement outcomes for all of the different values of m can be combined to infer θ (and hence a), and so to keep things general here we simply assume that the objective is to use the N_m shots to provide a point estimate of α_m, which we denote $\hat{\alpha}_m$. It is worth noting that this assumption, whilst simplistic, is likely to be sufficient to give a good guideline for how to increase the number of shots with m, certainly in the context of other assumptions that have already been made. We use the maximum likelihood estimate of α_m , which is simply the mean of the N_m samples, and using a Gaussian approximation of the binomial distribution, we get that our estimate of the amplitude is normally distributed according to:

$$\hat{\alpha}_m \sim \mathcal{N}\left(\alpha_m + \frac{1}{N_m}\sum_{i=1}^{N_m}\theta_\epsilon^{(i)}\sin((2m+1)\theta), \tilde{\sigma}^2\right) \tag{20}$$

where $\tilde{\sigma}^2 \leq 1/(4N_m)$, using the fact that a Bernoulli random variable has variance at most one quarter. However, when the mean of a Gaussian is itself normally distributed, it is easy to express the resultant distribution,

$$\hat{\alpha}_m \sim \mathcal{N}\left(\alpha_m, \frac{1}{N_m}\sigma^2 + \tilde{\sigma}^2\right) \tag{21}$$

If we let N_{shot} be the number of shots that would have been selected in the noiseless case (where $k_\sigma = 0$), then we can express the factor increase required to obtain the same estimation worst-case variance for the estimate of α_m:

$$\begin{aligned}\frac{1}{4N_{shot}} &= \frac{4k_\sigma m + 1}{4N_m} \\ \implies N_m &= (4k_\sigma m + 1)N_{shot}\end{aligned} \tag{22}$$

It is worth further remarking the sum in (20) can be thought of as further loop of summation of the errors, ϵ associated with *each* Grover iterate, (as in (3)) and hence "compounds" the use of the CLT, making the assumption of Gaussianity more plausible when the underlying noise model is used in this way.

VI. Noise-Aware QAE: Results

There are two ways in which a noise model can help to improve the accuracy of QAE: firstly by informing the experimental design, and secondly by improving the parameter inference. Bayesian adaptive methods essentially iterate over these two, and this would be an interesting future direction of research, however for now we treat the experiment as something that is designed in advance. In this case, the first of these items pertains to the ideas in the last section – that is, we can adjust the number of shots to approximately achieve the noiseless parameter estimation variance. For the second item, we can make use of the close connection between depolarising noise and our Gaussian noise model (*i.e.* assuming there is no bias, or if there is that it has been corrected by prior calibration) to use the N_m measurement outcomes to recover a typical instance of N_m measurement outcomes that we may have obtained without noise. In particular, we have that:

$$p(1) = \tilde{p}_{coh}^m \tilde{p}(1) + \frac{1}{2}(1-\tilde{p}_{coh}^m) \tag{23}$$

where as before $p(1)$ is the probability of measuring one in the presence of depolarising noise, and $\tilde{p} = \sin((2m+1)\theta)$ is the corresponding noiseless probability. This can easily be rearranged to give:

$$\tilde{p}(1) = \frac{1}{\tilde{p}_{coh}^m}(p(1) - \frac{1}{2}(1-\tilde{p}_{coh}^m)) \tag{24}$$

Thus, if we have $N^{(1)}$ "ones" amongst our N_m measurement outcomes, then we can project that we may have measured approximately $\frac{1}{\tilde{p}_{coh}^m}(N^{(1)} - \frac{1}{2}(1-\tilde{p}_{coh}^m))$ ones in the noiseless case.

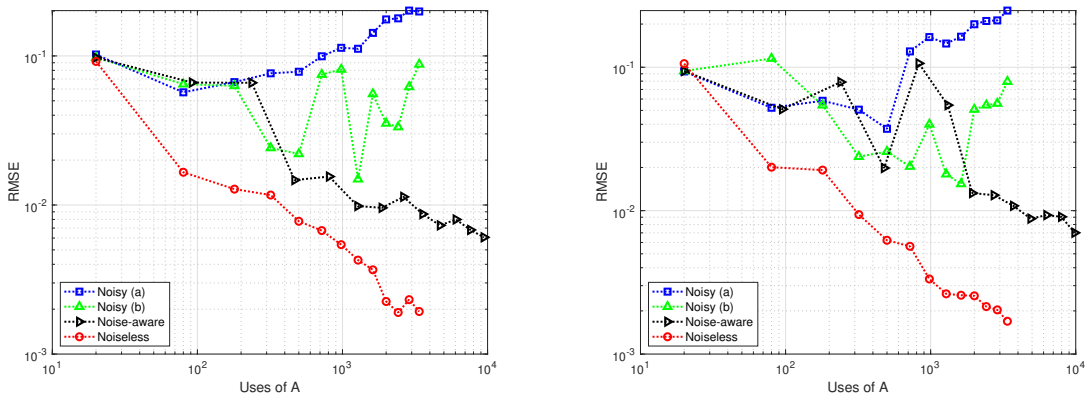

Fig. 7. QAE for various settings for the two experiments ((i) and (ii)) using Honeywell's machine: "noisy (a)", no use of the noise model; "noisy (b)", noise model uses only in parameter estimation; "noise-aware", noise model used in estimation and experimental design; and "noiseless", on a simulated ideal quantum computer.

We can use these two features to design a simple example of noise-aware QAE, based on the algorithm *Amplitude Estimation without Phase Estimation* proposed by Suzuki *et al* [12]. To do this, we re-use the results of the existing experiment running circuit A_5 on Honeywell's H1 trapped-ion quantum computer, and use the measurement outcome results for each of $\{0, 1, 2, 3, 4, 5, 6, 7, 8, 9, 10, 11, 12\}$ uses of A (this is a "linearly increasing sequence" in the terminology of Ref. [12]). As Suzuki *et al* only specify that a constant number of shots should be used for each element of the sequence, not a specific value, we choose 20 – which we will see is sufficient in the noiseless case. Even using only 20 shots, the data we collected only suffices to give us 14 independent runs of noise-aware QAE for (i) and 20 independent runs of noise-aware QAE for (ii) (that is, when the increase in N_m to counteract the noise is included), nevertheless this is enough to give us some indication of the benefits of noise-aware QAE. One may suggest that using data from the IBM experiments would be better, as more shots of each circuit were executed, however Honeywell has two distinct advantages: firstly, the much higher quantum volume gives us more interesting results (even *noise-aware* QAE can only do so much to lift results that dive into the noise floor almost immediately); and secondly, Honeywell was observed to have an almost zero bias (that is, $k_\mu \approx 0$), which eliminates the need for "calibration".

The second of these points, however, hints at something that we *do* need to do: that is, to use the measurement data to estimate the noise variance parameter, k_σ. The experimental limitations left us no option but to use the same data for this, which may suggest that we are cheating, however this is not in fact so: k_σ is a "coarse" parameter pertaining to the QAE as a whole, not any individual run (or even to the average of a large number of shots of some particular circuit consisting of some "m" uses of A_5). Moreover, it is reasonable to think that, as understanding of the noise characteristics of quantum computers matures, such a parameter will already been known from some generic device characterisation runs, and not from running QAE circuits as such.

We use the experimental data to compare four settings, as shown in Fig 7: QAE with $N_m = 20$, and no use of the noise model in the parameter estimation (labelled " noisy (a)"); QAE with $N_m = 20$, but where the noise model was used in the parameter estimation, *i.e.* in the sense of (24); noise-aware QAE where the noise model was used in both the parameter estimation *and* the experimental design – in this case, $N_m = 20, 24, 29, 33, 38, 42, 46, 51, 55, 60, 64, 68, 73$ and $N_m = 20, 25, 29, 34, 39, 44, 48, 53, 58, 62, 67, 72, 75$ for $m = 0, 1, \ldots 12$ for (i) and (ii) respectively (we omitted $m = 13$ for (ii) for consistency, and to be able to average over more runs); and finally, for comparison we simulated a noiseless quantum computer running QAE with $N_m = 20$.

As mentioned above, these results should be taken as indicative only, owing to the small number of QAE

runs, but nevertheless we can see the benefits of using the noise model. Without using the noise model at all (even in the parameter estimation) QAE completely fails to converge on the amplitude, whereas even with the noise model only used in the parameter estimation, some initial reduction in RMSE can be seen. However, we can clearly see that the convergence only continues if the noise model is used to adjust N_m such that more shots are executed when the inclement noise becomes more severe.

The final line, "noiseless" QAE, however, shows there is still some way to go. The challenge now is to use the proposed Gaussian noise model, together with ever-improving quantum hardware, to obtain compelling QAE results for problems of real-world interest. Furthermore, the linearly increasing sequence of Suzuki *et al* is known to not be optimal, and is only really used here for illustrative purposes. An important future line of research and development, therefore, will be to embed the noise model into other proposals for NISQ QAE to obtain noise-aware versions of the state-of-the-art NISQ QAE algorithms.

VII. Conclusions

In this paper we have proposed a simple Gaussian noise model that applies to NISQ QAE. We have run a number of experiments on various IBM superconducting quantum computers and Honeywell's H1 trapped-ion quantum computer to verify the model on real hardware. The proposed Gaussian noise model fits the experimental data well and, notably, captures the bias of the rotation angle, that the generic noise models do not. We have further shown how our proposed noise model can be used to inform the design of, and improve the parameter estimation in, QAE – yielding a first proposal for how to achieve noise-aware QAE.

Acknowledgement

The authors thank Cristina Cirstoiu for helpful conversations leading to the development and refinement of the theoretical model, and Ross Duncan for reviewing.

References

[1] J. Preskill, "Quantum computing in the NISQ era and beyond," *Quantum*, vol. 2, p. 79, Aug 2018. [Online]. Available: http://dx.doi.org/10.22331/q-2018-08-06-79

[2] K. Temme, S. Bravyi, and J. M. Gambetta, "Error mitigation for short-depth quantum circuits," *Physical Review Letters*, vol. 119, no. 18, Nov 2017. [Online]. Available: http://dx.doi.org/10.1103/PhysRevLett.119.180509

[3] Y. Li and S. C. Benjamin, "Efficient variational quantum simulator incorporating active error minimization," *Physical Review X*, vol. 7, no. 2, Jun 2017. [Online]. Available: http://dx.doi.org/10.1103/PhysRevX.7.021050

[4] J. J. Wallman and J. Emerson, "Noise tailoring for scalable quantum computation via randomized compiling," *Physical Review A*, vol. 94, no. 5, Nov 2016. [Online]. Available: http://dx.doi.org/10.1103/PhysRevA.94.052325

[5] S. Endo, S. C. Benjamin, and Y. Li, "Practical quantum error mitigation for near-future applications," *Physical Review X*, vol. 8, no. 3, Jul 2018. [Online]. Available: http://dx.doi.org/10.1103/PhysRevX.8.031027

[6] A. Holmes, M. R. Jokar, G. Pasandi, Y. Ding, M. Pedram, and F. T. Chong, "Nisq+: Boosting quantum computing power by approximating quantum error correction," in *2020 ACM/IEEE 47th Annual International Symposium on Computer Architecture (ISCA)*, 2020, pp. 556–569.

[7] R. Majumdar and S. Sur-Kolay, "Special session: Quantum error correction in near term systems," in *2020 IEEE 38th International Conference on Computer Design (ICCD)*, 2020, pp. 9–12.

[8] A. Montanaro, "Quantum speedup of monte carlo methods," *Proceedings of the Royal Society A: Mathematical, Physical and Engineering Sciences*, vol. 471, no. 2181, p. 20150301, 2015. [Online]. Available: https://royalsocietypublishing.org/doi/abs/10.1098/rspa.2015.0301

[9] F. G. S. L. Brandão, A. Kalev, T. Li, C. Y.-Y. Lin, K. M. Svore, and X. Wu, "Quantum sdp solvers: Large speed-ups, optimality, and applications to quantum learning," 2019.

[10] S. Aaronson and A. Arkhipov, "The computational complexity of linear optics," 2010.

[11] A. N. Chowdhury and R. D. Somma, "Quantum algorithms for gibbs sampling and hitting-time estimation," 2016.

[12] Y. Suzuki, S. Uno, R. Raymond, T. Tanaka, T. Onodera, and N. Yamamoto, "Amplitude estimation without phase estimation," *Quantum Information Processing*, vol. 19, no. 2, Jan 2020. [Online]. Available: http://dx.doi.org/10.1007/s11128-019-2565-2

[13] D. Grinko, J. Gacon, C. Zoufal, and S. Woerner, "Iterative quantum amplitude estimation," 2020.

[14] K. Nakaji, "Faster amplitude estimation," 2020.

[15] S. Aaronson and P. Rall, "Quantum approximate counting, simplified," *Symposium on Simplicity in Algorithms*, p. 24–32, Jan 2020. [Online]. Available: http://dx.doi.org/10.1137/1.9781611976014.5

[16] S. Herbert, "Quantum monte-carlo integration: The full advantage in minimal circuit depth," 2021.

[17] ——, "Quantum Computing System and Method: Patent application GB2102902.0 and SE2130060-3," 2021.

[18] D. An, N. Linden, J.-P. Liu, A. Montanaro, C. Shao, and J. Wang, "Quantum-accelerated multilevel monte carlo methods for stochastic differential equations in mathematical finance," 2020.

[19] P. Rebentrost, B. Gupt, and T. R. Bromley, "Quantum computational finance: Monte carlo pricing of financial derivatives," *Physical Review A*, vol. 98, no. 2, Aug 2018. [Online]. Available: http://dx.doi.org/10.1103/PhysRevA.98.022321

[20] N. Stamatopoulos, D. J. Egger, Y. Sun, C. Zoufal, R. Iten, N. Shen, and S. Woerner, "Option pricing using quantum computers," 2019.

[21] S. Woerner and D. J. Egger, "Quantum risk analysis," *npj Quantum Information*, vol. 5, no. 1, Feb 2019. [Online]. Available: http://dx.doi.org/10.1038/s41534-019-0130-6

[22] A. Bouland, W. van Dam, H. Joorati, I. Kerenidis, and A. Prakash, "Prospects and challenges of quantum finance," 2020.

[23] R. Orús, S. Mugel, and E. Lizaso, "Quantum computing for finance: Overview and prospects," *Reviews in Physics*, vol. 4, p. 100028, 2019. [Online]. Available: http://www.sciencedirect.com/science/article/pii/S2405428318300571

[24] D. J. Egger, R. G. Gutiérrez, J. C. Mestre, and S. Woerner, "Credit risk analysis using quantum computers," 2019.

[25] K. Kaneko, K. Miyamoto, N. Takeda, and K. Yoshino, "Quantum pricing with a smile: Implementation of local volatility model on quantum computer," 2020.

[26] S. Chakrabarti, R. Krishnakumar, G. Mazzola, N. Stamatopoulos, S. Woerner, and W. J. Zeng, "A threshold for quantum advantage in derivative pricing," 2020.

[27] P. Rebentrost and S. Lloyd, "Quantum computational finance: quantum algorithm for portfolio optimization," 2018.

[28] D. J. Egger, C. Gambella, J. Marecek, S. McFaddin, M. Mevissen, R. Raymond, A. Simonetto, S. Woerner, and E. Yndurain, "Quantum computing for finance: State-of-the-art and future prospects," *IEEE Transactions on Quantum Engineering*, vol. 1, pp. 1–24, 2020.

[29] J. Alcazar, A. Cadarso, A. Katabarwa, M. Mauri, B. Peropadre, G. Wang, and Y. Cao, "Quantum algorithm for credit valuation adjustments," 2021.

[30] E. G. Brown, O. Goktas, and W. K. Tham, "Quantum amplitude estimation in the presence of noise," 2020.

[31] T. Tanaka, Y. Suzuki, S. Uno, R. Raymond, T. Onodera, and N. Yamamoto, "Amplitude estimation via maximum likelihood on noisy quantum computer," 2020.

[32] T. Giurgica-Tiron, I. Kerenidis, F. Labib, A. Prakash, and W. Zeng, "Low depth algorithms for quantum amplitude estimation," 2020.

[33] I. Kerenidis and A. Prakash, "A method for amplitude estimation with noisy intermediate-scale quantum computers. U.S. Patent Application No. 16/892,229," 2020.

[34] G. Wang, D. E. Koh, P. D. Johnson, and Y. Cao, "Minimizing estimation runtime on noisy quantum computers," *PRX Quantum*, vol. 2, no. 1, Mar 2021. [Online]. Available: http://dx.doi.org/10.1103/PRXQuantum.2.010346

[35] P. Rao, K. Yu, H. Lim, D. Jin, and D. Choi, "Amplitude estimation algorithms and implementations on noisy intermediate-scale quantum devices," in *OSA Quantum 2.0 Conference*. Optical Society of America, 2020, p. QW6A.16. [Online]. Available: http://www.osapublishing.org/abstract.cfm?URI=QUANTUM-2020-QW6A.16

[36] G. Brassard, P. Hoyer, M. Mosca, and A. Tapp, "Quantum amplitude amplification and estimation," 2000.

[37] L. K. Grover, "A fast quantum mechanical algorithm for database search," in *Proceedings of the Twenty-Eighth Annual ACM Symposium on Theory of Computing*, ser. STOC '96. New York, NY, USA: Association for Computing Machinery, 1996, p. 212–219. [Online]. Available: https://doi.org/10.1145/237814.237866

[38] V. Garg, *Wireless Communications & Networking*, 1st ed. San Francisco, CA, USA: Morgan Kaufmann Publishers Inc., 2007.

[39] "IBM quantum computing." [Online]. Available: https://www.ibm.com/quantum-computing

[40] "TKET." [Online]. Available: https://github.com/CQCL

[41] "Honeywell quantum solutions." [Online]. Available: https://www.honeywell.com/us/en/company/quantum

[42] "Honeywell quantum volume." [Online]. Available: https://www.honeywell.com/us/en/news/2021/03/honeywell-sets-new-record-for-quantum-computing-performance

Appendix A. Compiled Circuits

In this appendix we give compiled circuits for A_1, A_2, A_3, A_4, A_5.

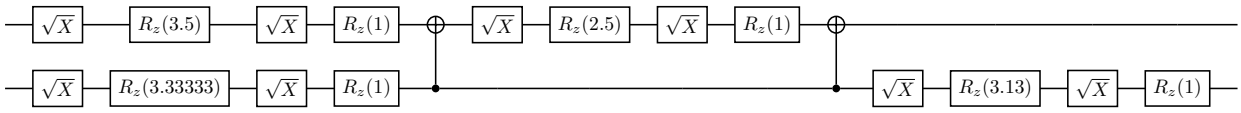

A_1 compiled for IBM

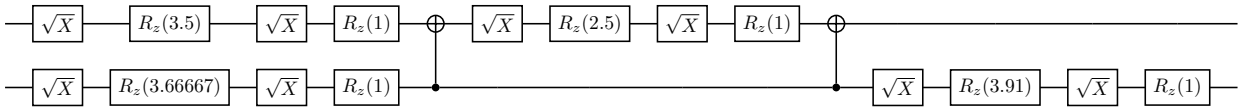

A_2 compiled for IBM

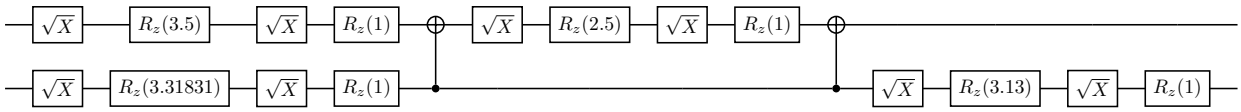

A_3 compiled for IBM

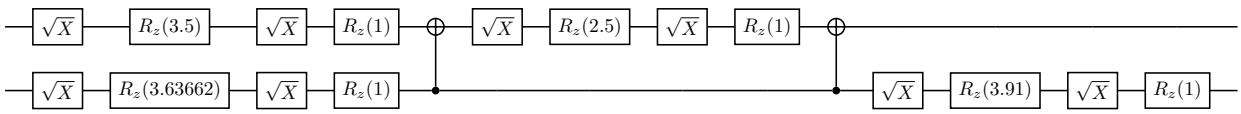

A_4 compiled for IBM

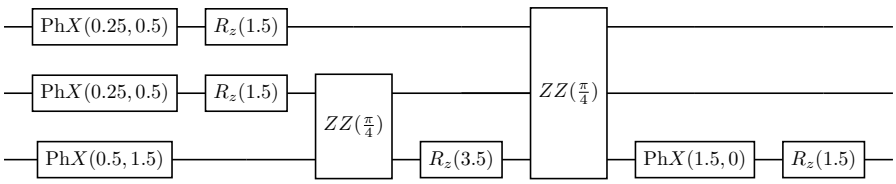

A_5 compiled for Honeywell H1